


Proceedings Article

# MNP Characterization and Signal Prediction using a Model-Based Dictionary

Asli Alpman <sup>a,b,\*</sup>, Mustafa Utkur <sup>a,b</sup>, Emine Ulku Saritas <sup>a,b,c</sup>

<sup>a</sup>Department of Electrical and Electronics Engineering, Bilkent University, Ankara, Turkey

<sup>b</sup>National Magnetic Resonance Research Center (UMRAM), Bilkent University, Ankara, Turkey

<sup>c</sup>Neuroscience Program, Sabuncu Brain Research Center, Bilkent University, Ankara, Turkey

\*Corresponding author, email: [alpman@ee.bilkent.edu.tr](mailto:alpman@ee.bilkent.edu.tr)

© 2022 Alpman *et al.*; licensee Infinite Science Publishing GmbH

This is an Open Access article distributed under the terms of the Creative Commons Attribution License (<http://creativecommons.org/licenses/by/4.0>), which permits unrestricted use, distribution, and reproduction in any medium, provided the original work is properly cited.

## Abstract

Magnetic Particle Imaging (MPI) utilizes the nonlinear magnetic response of magnetic nanoparticles (MNPs) for signal localization. Accurate modeling of the magnetization behavior of MNPs is crucial for understanding their MPI signal responses. In this work, we propose a model-based dictionary approach using a coupled Brown-Néel rotation model. With experimental results on a Magnetic Particle Spectrometer (MPS), we show that this approach can successfully characterize MNP parameters and predict signal responses.

## I. Introduction

In Magnetic Particle Imaging (MPI), the magnetization response of magnetic nanoparticles (MNPs) is governed by two main mechanisms: Néel and Brownian rotations. While the Brownian process physically rotates the MNP to align its magnetic moment with the applied field, the Néel process flips the magnetic moment internally [1].

The Brownian and Néel mechanisms occur in a coupled fashion, where the physical rotation of the MNP and the internal rotation of the magnetic moment affect each other. Accurate modeling of these mechanisms is essential for characterizing MNPs and understanding their MPI responses. Previously, model-based simulation approaches have been utilized for such purposes [2–4].

In this study, we propose a model-based dictionary approach to characterize MNPs and predict their signal responses using a Magnetic Particle Spectrometer (MPS). To accurately characterize the MNP, we use a coupled Brown-Néel rotation model and include the signals of the same MNP at different viscosity levels at a single drive field (DF) setting in our dictionary. Further, we show

that this approach can successfully predict the signal responses of the characterized MNP at viscosity levels that are not included in the characterization step.

## II. Materials and Methods

### II.1. Dictionary Preparation

The magnetic responses of the MNPs with various magnetic properties and viscosity levels were simulated at DF settings of 10 mT and 250 Hz, by solving an ordinary differential equation (ODE) using MATLAB. The ODE, taken from [5], was derived from the Fokker-Planck equation for coupled Brown-Néel rotation, assuming single-core, non-interacting particles with uniaxial magnetic anisotropy and uniaxial symmetry.

The dictionary included MNPs with core diameters ( $d_c$ ) ranging from 10 nm to 25 nm, hydrodynamic diameters ( $d_h$ ) from 25 nm to 125 nm, uniaxial magnetic anisotropy constants ( $K$ ) from  $1 \text{ kJ m}^{-3}$  to  $14 \text{ kJ m}^{-3}$ , and 5 different viscosity levels ( $\eta$ ) from  $0.893 \text{ mPa} \cdot \text{s}$  to  $8.312 \text{ mPa} \cdot \text{s}$ . Saturation magnetization, Gilbert damp-

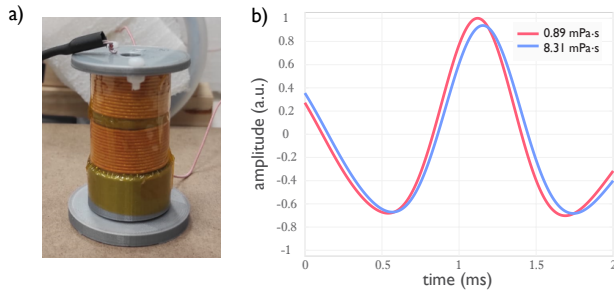


**Figure 1:** (a) In-house arbitrary waveform MPS setup. (b) Example half period signals for 0.89 mPa·s and 8.31 mPa·s samples at 10 mT and 250 Hz DF settings.

ing constant, and temperature were assumed to be 360 kA/m, 0.1, and 25°C, respectively.

## II.II. Inverse Problem Formulation

Assuming that the measured MNP signal can be expressed as a weighted linear combination of the simulated MNP signals, an inverse problem was formulated. The weights of this linear combination enabled us to characterize the MNPs.

We created a dictionary matrix containing MNP responses at 5 different viscosity level at the chosen DF settings of 10 mT and 250 Hz. The problem was formulated in the frequency domain by selecting the odd harmonics with magnitudes higher than the noise floor. We formulated the problem as a least squares problem with non-negativity and sparsity constraints, i.e.,

$$\min_{x \in \mathbb{R}^n} \|Ax - b\|_2^2 + \lambda \|x\|_1 \quad \text{s.t.} \quad x \geq 0 \quad (1)$$

where  $A$  is the dictionary matrix,  $b$  is the vector with concatenated experimental data from different viscosity levels,  $n$  is the number of particles in the dictionary,  $x$  is the vector of weights characterizing the MNP, and  $\lambda$  is a scalar weight for  $\ell_1$ -norm. We used the Alternating Direction Method of Multipliers (ADMM) to solve this optimization problem.

For the signal prediction task, the characterization step excluded the corresponding dictionary components and measured signals from  $A$  and  $b$ , respectively. As a quantitative evaluation metric, normalized root mean square error (NRMSE) is utilized:

$$\text{NRMSE}(x, \hat{x}) = \frac{\sqrt{\frac{\sum_{i=1}^N (x_i - \hat{x}_i)^2}{N}}}{\max_i x_i - \min_i x_i} \quad (2)$$

Here,  $N$  is the number of samples in one period of the signal,  $x$  and  $\hat{x}$  are the measured and predicted signals for the sample excluded from the dictionary.

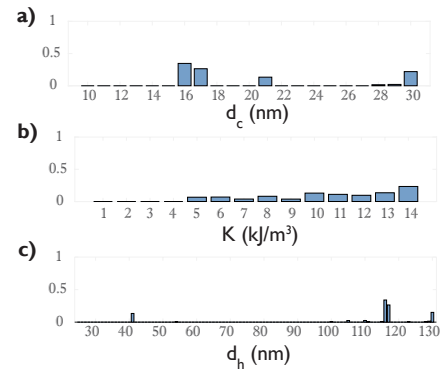


**Figure 2:** Magnetic characterization results for PrecisionMRX, displaying the probability mass functions for (a)  $d_c$ , (b)  $K$ , and (c)  $d_h$ . Samples at 5 different viscosity levels were measured at 10 mT and 250 Hz DF settings to obtain these results.

**Table 1:** Glycerol volume percentages at 25°C for samples at 5 different viscosity levels. Each sample contained 26.2  $\mu$ l of PrecisionMRX.

| Viscosity (mPa·s)        | 0.89 | 1.45 | 2.08 | 3.32 | 8.31 |
|--------------------------|------|------|------|------|------|
| Glycerol (% vol at 25°C) | 0    | 15.1 | 24.8 | 35.7 | 53.2 |

## II.III. MPS Experiments

Experiments were performed on an in-house arbitrary waveform MPS setup (see Fig. 1). The DF waveform was sent to the power amplifier (AE Techron 7224) via a data acquisition card (NI USB-6383). A low-noise amplifier (SRS SR560) amplified the MNP signal induced on the two-section gradiometric receive coil. The experiments were conducted at 10 mT and 250 Hz DF settings on samples at 5 different viscosity levels (see Table 1). Each experiment was repeated 3 times. Each sample had a total volume of 70  $\mu$ l, with varying volumes of glycerol and deionized water [6]. All samples contained 26.2  $\mu$ l of PrecisionMRX nanoparticles (Imagion Biosystems Inc., USA), which are single-core MNPs with 25 nm core diameter and 40 nm hydrodynamic diameter, according to their data sheet.

## III. Results and Discussion

Figure 2 shows the characterization results using samples at all 5 viscosity levels. The pronounced peak around 17 nm for  $d_c$  is consistent with the previous characterization work [7]. Also, the results show a small peak around 40 nm for  $d_h$ , which is consistent with  $d_h$  given by the manufacturer. Although PrecisionMRX is reported to contain single-core MNPs, we observe a polydisperse nature in  $d_c$  in the characterization results. This discrepancy may be caused by the non-idealities in the system, the magnetization model, or the MNPs. First, the non-idealities of the system can distort the MNP signal, and

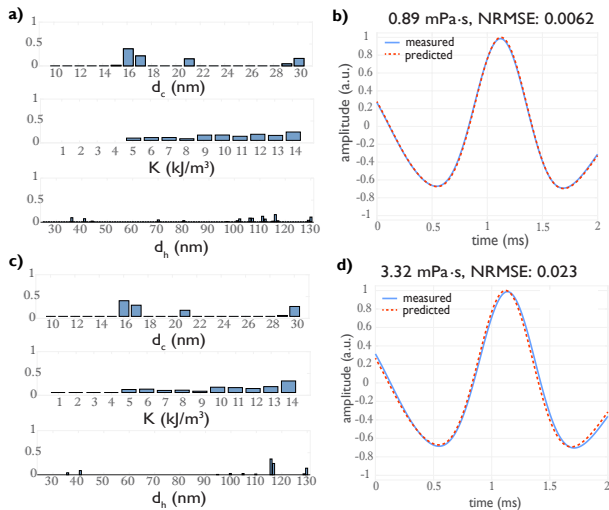


**Figure 3:** Signal prediction results. (a) Magnetic characterization for PrecisionMRX when 0.89 mPa·s sample is left out, and (b) the predicted vs. measured signals for that sample. (c) Magnetic characterization for PrecisionMRX when 3.32 mPa·s sample is left out, and (d) the predicted vs. measured signals for that sample.

the solution of the inverse problem may compensate for this distortion by adding physically non-existing MNPs to  $x$ . Secondly, the magnetization model that we used assumed uniaxial symmetry and uniaxial anisotropy, which may not strictly hold for the tested MNPs. Lastly,  $d_c$  and  $d_h$  values, which have distinct peaks at higher values than the ones reported by the previous work or the data sheet, can be a sign of agglomeration of the MNP.

Figure 3 shows the signal prediction capability of the model. For each viscosity level of interest, the measured and predicted signals are shown, together with the MNP characterization results using the remaining 4 viscosity levels. The characterization results (i.e., the overall distributions for  $d_c$ ,  $K$ , and  $d_h$ ) do not change substantially when different viscosity levels are excluded, showing the robustness of the characterization procedure. Furthermore, for each case, the predicted signal using the characterization from the remaining 4 viscosity levels provides a close match to the measured signal, together with a low NRMSE.

Figure 4 shows that the NRMSE for the signal prediction remains below 6% at all viscosity levels. As expected, the prediction performance improves when viscosity levels close to the targeted one are included in the characterization step. For example, the NRMSE value for the predicted signal at 8.312 mPa·s is the highest, since its viscosity value is the furthest away from the others.

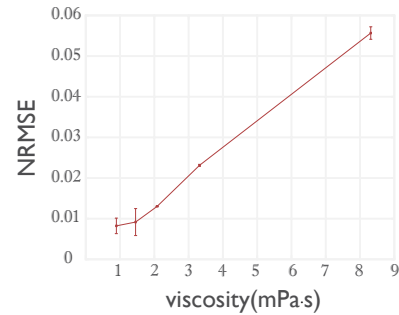


**Figure 4:** NRMSE of the predicted signals for 5 different viscosity levels. In each case, the viscosity level of interest was left out during the characterization step. The error bars show the standard deviation across 3 repetitions.

## IV. Conclusion

This work proposes a framework to characterize MNP parameters and predict signal responses using a model-based dictionary approach. The qualitative and quantitative assessments demonstrate successful signal prediction for single-core MNPs using a coupled Brownian-Néel model. The proposed signal prediction approach is expected to have important applications, such as viscosity mapping and temperature mapping using MPI.

## Acknowledgments

This work was supported by the Scientific and Technological Research Council of Turkey (Grant No: TUBITAK 120E208).

## Author's statement

Conflict of interest: Authors state no conflict of interest.

## References

- [1] C. Shasha and K. Krishnan. Nonequilibrium dynamics of magnetic nanoparticles with applications in biomedicine. *Advanced Materials*, 33:1904131, 2020, doi:[10.1002/adma.201904131](https://doi.org/10.1002/adma.201904131).
- [2] A. Neumann, S. Draack, F. Ludwig, and T. M. Buzug. Parameter estimations of magnetic particles: A comparison between measurements and simulations, in *International Workshop on Magnetic Particle Imaging*, 79, 2019.
- [3] D. V. Berkov, P. Görnert, N. Buske, C. Gansau, J. Mueller, M. Giersig, W. Neumann, and D. Su. New method for the determination of the particle magnetic moment distribution in a ferrofluid. *Journal of Applied Physics*, 33(4):331–337, 2000, doi:[10.1088/0022-3727/33/4/303](https://doi.org/10.1088/0022-3727/33/4/303).
- [4] H. Albers, T. Kluth, and T. Knopp. Simulating magnetization dynamics of large ensembles of single domain nanoparticles: Numerical study of brown/néel dynamics and parameter identification problems in magnetic particle imaging. *Journal of Magnetism and Magnetic Materials*, 541:168508, 2022, doi:<https://doi.org/10.1016/j.jmmm.2021.168508>.

- [5] J. Weizenecker. The fokker–planck equation for coupled brown–néel-rotation. *Physics in Medicine & Biology*, 63(3):035004, 2018, doi:[10.1088/1361-6560/aaa186](https://doi.org/10.1088/1361-6560/aaa186).
- [6] N.-S. Cheng. Formula for the viscosity of glycerol water mixture. *Industrial Engineering Chemistry Research*, 47(9):3285–3288, 2008, doi:[10.1021/ie071349z](https://doi.org/10.1021/ie071349z).
- [7] O. L. Lanier, O. I. Korotych, A. G. Monsalve, D. Wable, S. Savliwala, N. W. F. Grooms, C. Nacea, O. R. Tuitt, and J. Dobson. Evaluation of magnetic nanoparticles for magnetic fluid hyperthermia. *International Journal of Hyperthermia*, 36(1):686–700, 2019, PMID: 31340687. doi:[10.1080/02656736.2019.1628313](https://doi.org/10.1080/02656736.2019.1628313).